# AIR SPARGING EXPERIMENTS ON A TWO DIMENSIONAL SAND BOX WITH DNAPLS: MULTIPHASE INVESTIGATION WITH ELECTRICAL IMPEDANCE TOMOGRAPHY

Jong Soo Cho

US Environmental Protection Agency

National Risk Management Research Laboratory

Subsurface Processes and Remediation Division, Ada, Oklahoma

## ABSTRACT

Electrical impedance tomography (EIT) applications in detection of organic chemical sources and monitoring subsurface environments during air-sparging were studied. The development of an inverse solution program and experimental tests in the laboratory were included in this study. The inverse solution model used the Newton-Raphson method with the Marquadt regularization technique. A multiphase flow and transport model was utilized to test the EIT inverse modeling. Tetrachloroethylene (PCE) infiltration was simulated with a multiphase flow model and the ability of EIT to trace the PCE distribution was tested. Computational progress of the inverse solution was presented with a graphical display of electrical conductivity distributions. The inverse program for EIT was used to obtain the electrical conductivity distribution in a 2-D sand box. The experiments included a spillage of dense non-aqueous phase liquid (DNAPL) dyed with a hydrophobic dye at the top of the sand box filled with water and air sparging from the bottom. Electrical conductivity changed in the soil as water was replaced water with DNAPL or air. This made the tomographic pictures of electrical conductivity. The vapor concentration of DNAPL in the extracted air was measured

1

with a GC to estimate the removal rate during air sparging . The tomographic images from the EIT were compared with photographic images of dyed PCE in the water filled space.

## INTRODUCTION

The Electrical Impedance Tomography has been used widely by geophysicists (Tripp et al, 1984) to detect geological anomalies in the subsurface and by mining engineers (Shima, 1992) to locate mineral cores. Recently, biomedical engineers (Yorkey et al, 1985) started the application of this technique to monitor their patients. The major advantage of EIT in medical application is that it is much less harmful than X-ray or any isotope intake methods. In environmental areas, this technique has been applied to locate the leakage from lined wastewater treatment ponds (Van et al, 1991), to monitor the infiltration of water through subsurface (Daily et al, 1992), and to trace the steam propagation during remediation with steam injection (Ramirez et al, 1993). Due to electrical impedance differences of various phases of fluids in the subsurface, i.e. air, water, and NAPLs, it was possible to monitor the movement of the separate phases of fluid in the subsurface.

The basic principle of the EIT is that the electrical current passes through the less resistive section bypassing the more resistive locations. By measuring the potential/current distribution in space, differences in the conductivity distribution can be detected by inverting the measured potential/current distribution with the computer programs. The electrical conductivity of pure water is $4.2 \times 10^{-2}$ Scm$^{-1}$ at 25 °C and commonly available distilled water has electrical conductivities in the range of 0.5 to 5 Scm$^{-1}$. The electrical conductivity of fresh ground water is in the range of 30 to 2000 Scm$^{-1}$; for PCE, a nonelectrolytic organic solvent, it is $1 \times 10^{-9}$ Scm$^{-1}$. Air is a very good insulator. The relationship between the resistivity and soil moisture content

2

can be expressed with Archies' law (Archies, 1942):

$$\rho = a\rho_w \phi^{-m} \tag{1}$$

where $\rho$ is the bulk resistivity, $\rho_w$ is the resistivity of the pore water, $\phi$ is the volume fraction porosity, and $a$ and $m$ are fitting parameters ($a$=1, $m$ = 1.3 - 1.5 for unconsolidated sand, Barber et al. 1991). The following modification can be applied to the partially saturated media:

$$\rho = S^{-n}(a\rho_w \phi^{-m}) \tag{2}$$

where $S$ is the fraction water saturation and $n$ is empirically determined but is usually $2 \pm 0.5$ (Hearst and Nelson, 1985). The electrical resistivity of a sandy aquifer material partially filled with DNAPL was reported by Annan et al. (1991) and Schneider and Greenhouse (1994). The estimated electrical resistivity in the sand partially filled with PCE and water is listed in table 1. The parameters used for the estimation were: soil porosity, 0.4; electrical resistivity of PCE, $\infty$; water resistivity, 20 $\Omega$m; constants in the Archies' law equation, $a$=1.0, $n$=2.0, and $m$=1.0.

## INVERSE MODEL FOR EIT

The electrical field in conductive media can be described by a Poisson's equation

$$\nabla \cdot k\nabla V = -f \tag{3}$$

with boundary conditions

$$V = V_o \quad on \quad \partial A \tag{4}$$

$$k\frac{\partial V}{\partial n} = J_o \qquad on \quad \partial A \tag{5}$$

where $k$, $V$, and $f$ are the conductivity, voltage, and impressed current source distribution, and $\nabla$ is the Laplacian operator, and $A$ is the boundary. The forward solution of the above equation is to find the internal voltages and current densities with known conductivity distribution and boundary conditions. The inverse solution is to find the conductivity distribution which can produce measured voltage and current density distribution on the boundaries and internal space. The inverse solution is actually an iteration of forward solutions with assumed conductivity distributions. The forward solution is repeated until the objective function, usually the summation of squared errors, meets the criteria. At each iteration, the parameters, here the conductivity distribution, are adjusted in the direction of reducing errors. The direction of the parameter adjustment is searched by the non-linear parameter optimization method. In this effort, the Newton-Raphson method (Hua and Woo, 1990) is used (Figure 1).

Newton-Raphson Method

The objective function is defined as

$$\Phi(k) = 1/2(V(k) - V_o)^T(V(k) - V_o) \tag{6}$$

where $V_o$ is the measured voltage, $V(k)$ the computed voltage for a conductivity distribution $k$. To find the $k$ which minimizes the objective function, its derivative is expressed as

$$\Phi'(k) = [V'(k)]^T(V(k) - V_o) = 0 \tag{7}$$

Taylor series expansion yields

4

$$\Phi'(k^{k+1}) = \Phi'(k^h) + \Phi''(k^h)\Delta k^k \qquad (8)$$

where $k^{k+1} = k^k + \Delta k^k$. The term $\Phi''$ is called the Hessian matrix,

$$\Phi'' = (V')^T V' + (V'')^T [I \otimes (V - V_o)] \qquad (9)$$

Truncating the second derivative term, it becomes

$$\Phi'' = (V')^T V' \qquad (10)$$

Substitution of equations yields,

$$[(V')^T V'] \Delta k^k = -(V')^T [V - V_o] \qquad (11)$$

## Regularization

Due to the ill-posed condition on the Hessian matrix, the Marquadt method (Marquadt, 1963) was adopted. The equation (11) is written in a matrix/vector form as

$$[H][\Delta k] = [g] \qquad (12)$$

where [g] represents the right hand side of the equation (11). By adding a stabilization term after scaling the matrix and vectors, it becomes

$$[H^* + \lambda I][\Delta k^*] = [g^*] \qquad (13)$$

where $\lambda$ is an arbitrary positive constant, $I$, the identity matrix. Hessian matrix and vectors are scaled as:

5

$$[H^*] = [\frac{H_{ij}}{\sqrt{H_{ii}}\sqrt{H_{jj}}}]$$ (14)

$$[g^*] = [\frac{g_i}{\sqrt{H_{ii}}}]$$ (15)

and

$$[\Delta k] = [\frac{k_j^*}{\sqrt{H_{jj}}}]$$ (16)

## Finite Difference Formulation

A five-point finite difference approximation of the Poisson's equation in the 2D rectangular space is

$$\frac{1}{\Delta x}(\frac{k_{x+1y}+k_{xy}}{2}\frac{V_{x+1y}-V_{xy}}{\Delta x} - \frac{k_{xy}+k_{x-1y}}{2}\frac{V_{xy}-V_{x-1y}}{\Delta x}) +$$
$$\frac{1}{\Delta y}(\frac{k_{xy+1}+k_{xy}}{2}\frac{V_{xy+1}-V_{xy}}{\Delta y} - \frac{k_{xy}+k_{xy-1}}{2}\frac{V_{xy}-V_{xy-1}}{\Delta y}) = -f_{xy}$$ (17)

which is in a matrix format

$$[A][V] = [B]$$ (18)

where $[A]$ is the coefficient matrix, and $[V]$ and $[B]$ are the vectors of potentials and impressed currents.

6

Sensitivity Matrix

The relationship between changes in model parameters and results of the model

(McGillivray and Oldenburg, 1990) is expressed by

$$V_{ij}' = \frac{\partial V_i}{\partial k_j} \tag{19}$$

Differentiation of the difference equation on both sides with $k_j$ yields

$$[A]'[V] + [A][V]' = 0 \tag{20}$$

which becomes

$$[A][V]' = -[A]'[V] \tag{21}$$

The equation (21) has the identical coefficient matrix [ A ] with the matrix difference equation

(18). Once the coefficient matrix [ A ] is obtained, then the same solution process can be

repeated to obtain the [V]'. For the five- point difference formulation, only thirteen elements in

[ A ]' have non-zero values for differentiation with $k_j$.

## NUMERICAL TESTING

An aquifer highly contaminated by nonaqueous phase liquid has four primary phases: a

stationary phase composed primarily of mineral soil and organic matter, an aqueous phase

consisting of water and dissolved ions, a vapor phase consisting primarily of air, and a non-

aqueous phase normally consisting of organic liquids. It is assumed that the electrical properties

of the aqueous phase are not significantly changed as the organic components of limited

7

solubilities are dissolved. The observed change is assumed to be a result of the volume fraction occupied by each phase. Tetrachloroethylene (PCE) has been used as a solvent in machine shops and dry cleaning facilities. Since PCE is a chlorinated hydrocarbon which is heavier and less viscose than water with a specific gravity, 1.63 and relative viscosity, 0.9, it can infiltrate below the water table and serve as a long-term source for ground-water contamination. From the bottom of the aquifer, detection and removal of PCE become very difficult.

A simulation of PCE infiltration in a 2D sand box was conducted with a multiphase fluid flow model (MOFAT, 1991) and detection of electrical conductivity change using the EIT inverse was examined. The parameters used in the simulation are in Table 2. The initial water and electrical conductivity distribution are seen in Figure 2. These were used as the baseline information. The water table located at 15 cm below the surface. The electrical conductivity shows a very similar pattern. Water saturation at 0.4 hr after a PCE spill at the top of the sand box shows tremendous changes due to PCE infiltration (Figure 3). PCE started to touch the bottom of the sand box and both side walls at this moment. Electrical conductivity distribution followed very closely the pattern of water saturation. The EIT inverse model was tested to see whether it could trace the conductivity pattern. Five electrical nodes were located on both sides of the sand box at a depth of 5, 10, 15, 20, and 25 cm. The total number of voltage measurement at the electrodes was three hundred fifteen with 169 unknown values of conductivities. Uniform distribution of conductivity was used as the initial guess in the inverse model. After 10 iterations, the sum of squared errors reduced from 1.16 to $8.73 \times 10^{-3}$ and became $3.9 \times 10^{-5}$ after the 27th iteration (Figure 4). Most of the computation time was spent on sensitivity matrix calculations at each iteration.

## SAND BOX EXPERIMENTS

A 2D sand box was built of Teflon® square bars, glass, and plexiglass plates (Figure 5). The size of the sand box was 70 cm x 50 cm with 2.5 cm thickness. It was mounted on wooden brackets inside a ventilation hood in the laboratory. To make tight seals between glass plates and frame bars, Teflon® joint sealant and vise grips were used. Seven ½ inch holes were drilled and threaded to install the Teflon® compression fittings on both side frames. One hole was drilled at the bottom bar for the air-sparging tubing and the Teflon® compression fittings were installed. Five electrodes made of 1/4 inch copper coated carbon rods were inserted through the fittings. One hole on each side was used as the water intake and outlet port. The sand box was initially filled with sand and tap water. Later the spill of PCE from the top and the air-sparging from the bottom were initiated.

Experimental data were obtained using electrodes and the multimeter connected through rotary switches. The four-electrode method was used to eliminate the electrical noise caused by the electrochemical reaction around the current electrodes. A constant current (0.33 mA) was passed through two electrodes. The third electrode was used as the reference electrode for the potential measurement. This setting yields $n(n-1)/2$ independent voltage measurements sets with n electrodes. All of the measurements were done with a multimeter and manual rotary switches. Three hundred fifteen voltage measurements for an individual cycle were expected.

The electrical parts used in the experiment were as follows: ten carbon electrodes, five on the each side of the sandbox; a 15 V power supply; a low distortion oscillator; a constant current circuit board to supply 0.33 mA current; a switch board connected to the power supply, oscillator, circuit and electrodes, complete with four different adjustments (injection node,

9

reference node, extraction node, and voltage node); and a multimeter. The physical measurement components were a rotameter and a pressure gauge for air flow.

Data are being collected at the present time under various sand box conditions with PCE and air. They will be used as the input data files for the inverse model. Output generated from the inverse model will be sent to a visualization software (Geomview, 1993) to produce graphical outputs.

## RESULTS AND DISCUSSION

From the comparison of conductivity distribution before and after the PCE spill, very distinctive differences could be found. This difference allowed EIT to trace the separate phase liquid movement. Testing of the EIT inverse model showed that the model could minimize the object function by several orders of magnitude, but the model still needs further tuning for accurate tracing and reduction of noise expected during the potential measurement. Next step is the actual application of the EIT in the laboratory experiment with a sand box. Measurement noises in the experiments are expected and the robustness of the EIT inverse model should be tested against them. The images of the electrical conductivity distribution generated from the EIT inverse mode will be compared with the photographic images from dyed chemical distribution inside the sand box.

## CONCLUSIONS

1. Change of electrical resistivity could be found during the PCE infiltration in the simulation with a multiphase flow model.

2. The EIT tests with the simulation results showed its ability to detect the anomalies of electrical conductivities. The developed program showed its ability to locate the anomalies even

though the absolute values of conductivity estimated showed marginal errors, especially at the boundaries. The inverse model still needs further adjustments.

3. The most computation time in the inverse modeling was spent in the calculation of sensitivity matrices. Other methods such as the compensation theory method will significantly reduce the computational time.

3. The Newton-Raphson method with the Marquadt regularization showed a good computational efficiency and stability. With significant measurement noise, the regularization method will help to reduce the instability problems.

4. The 2-D EIT inverse model will be used to investigate the DNAPL and air movement in the laboratory experiments.

## DISCLAIMER

Although the research reported in this paper has been funded wholly or in part by the United States Environmental Protection Agency, it has not been subjected to the agency peer-review and therefore does not necessarily reflect the view of the agency. No official endorsement of the system design or trade names should be inferred.

## REFERENCES

Annan, A. P., P. Bauman, J.P. Greenhouse, and J.D. Redman, 1991, Geophysics and DNAPLS: Groundwater Management #5, in Proc. of the Fifth Annual Outdoor Action Conference on Aquifer Restoration, Groundwater Monitoring, and Geophysical Methods, Las Vegas, Nevada.

Archies, G.E., 1942, The Electrical Resistivity Log as an Aid in Determining Some Reservoir Characteristics, *Trans. Am. Inst. Min. Metall. Pet. Eng.*, **146**, 54.

Barber, C., G.B. Davis. G. Buselli, and M. Height, 1991, Remote Monitoring of Groundwater Pollution Using Geoelectric Techniques in Undulating Sandy Terrain, Western Australia, *International Journal of Environment and Pollution*, **1**(½), 97-112.

Daily, W., A.Ramirez, D.Labreque, and J.Nitao, 1992, Electrical Resistivity Tomography of

Vadose Water Movement, *Water Resources Research*, **28**(5), 1429-1442.

Geomview®, 1993, Geomview Manual, The Geometry Center, University of Minnesota, Minneapolis, MN.

Hearst, J.R. and P.H. Nelson, 1985, Well Logging for Geophysical Properties, MacGraw-Hill, New York, NY.

Hua, P. and E.J. Woo, 1990, Chapter 10, Reconstruction Algorithms, Electrical Impedance Tomography, edited by J.G.Webster, Adam Hilger, Bristol and New York.

Marquadt, D.W., 1963, An Algorithm for Least-Squares Estimation of Nonlinear Parameters, *J. Soc. Indust. Appl. Math.*, **11**(2), 431-441.

McGillivray, P.R. and D.W.Oldenburg, 1990, Methods for Calculating Frechet Derivatives and Sensitivities for the Non-Linear Inverse Problem: A Comparative Study, *Geophysical Prospecting*, **38**, 499-524.

MOFAT, A Two-Dimensional Finite Element Program for Multiphase Flow and Multicomponent Transport, Program Documentation and User's Guide, EPA/600/2-91/020, US EPA, RSKERL, Ada, OK, 1991.

Ramirez, A., W. Daily, D.Labreque, E.Owen, and D.Chesnut, 1993, Monitoring an Underground Steam Injection Process Using Electrical Resistance Tomography, *Water Resources Research*, **29**(1), 73-87.

Schneider, G.W. and J.P. Greenhouse, 1994, Geophysical Detection of Perchloroethylene in a Sandy Aquifer Using Resistivity and Nuclear Logging Techniques, in Proc. of Symposium on the Application of Geophysics to Engineering & Environmental Problems, Atlanta, GA.

Shima, H., 1992, 2-D and 3-D Resistivity Image Reconstruction Using Crosshole Data, *Geophysics*, **57**(10), 1270-1281.

Tripp, A.C., G.W. Hohman, and C.M. Swift,Jr., 1984, Two Dimensional Resistivity Inversion, *Geophysics*, **49**(10), 1708-1717.

Van, G.P., S.K. Park, and P. Hamilton, 1991, Monitoring Leaks from Storage Ponds Using Resistivity Methods, *Geophysics*, **56**(8), 1267-1270.

Yorkey, T.J., J.G. Webster, and W.J. Tompkins, 1987, Comparing Reconstruction Algorithms for Electrical Impedance Tomography, *IEEE Transactions on Biomedical Engineering*, **BME-34**(11), 843-852.

**Table 1. Electrical Resistivity in the Sand Partially Filled with PCE and Water**

| Saturation of PCE (%) | Resistivity ($\Omega$m) |
|---|---|
| 0.0 | 72 |
| 10 | 89 |
| 20 | 113 |
| 50 | 289 |
| 75 | 1154 |
| 90 | 7200 |
| 100 | $\infty$ |

**Table 2. Parameters Used in the Multiphase Model Simulation and Inverse Model**

| | | |
|---|---|---|
| PCE Properties | Density | 1.63 g/cm$^3$ |
| | Viscosity | 0.9 cp |
| Soil Properties | Porosity | 0.4 |
| | Hydraulic Conductivity | 40 cm/hr |
| Van Genuchten Parameters | $\alpha$ | 0.145 cm$^{-1}$ |
| | n | 2.8 |
| | $S_m$ | 0.1 |
| | $S_{row}$ | 0.2 |
| Sand Box Dimension | Size | 30 x 30 x 1 cm |
| | Initial Water Table | 15 cm |
| | Initial Water Volume | 301 cm3 |
| PCE Infiltration | Infiltration Mode | Constant Head |
| | Infiltration Period | 0.28 hr (17 min) |
| | Total Volume | 36 cm$^3$ |
| EIT Inverse Model | Nodes (Unknown Conductivities) | 13 x 13 (169) |
| | Electric Nodes | 10 |
| | Time of Measurement | 0.4 hr (24 min) |
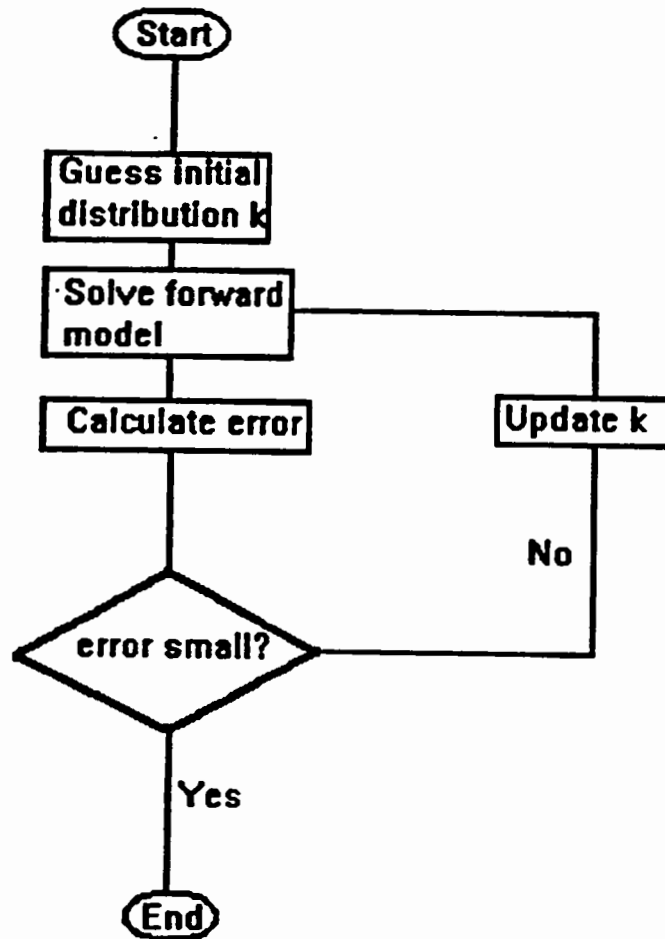
**Figure 1. Flow Chart of Inverse Solution algorithm for Electrical Impedance Tomography**
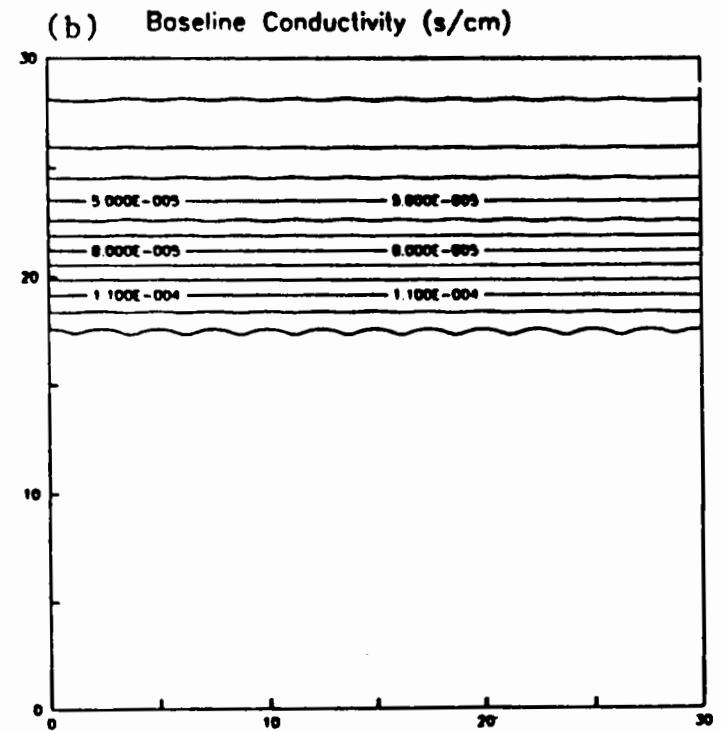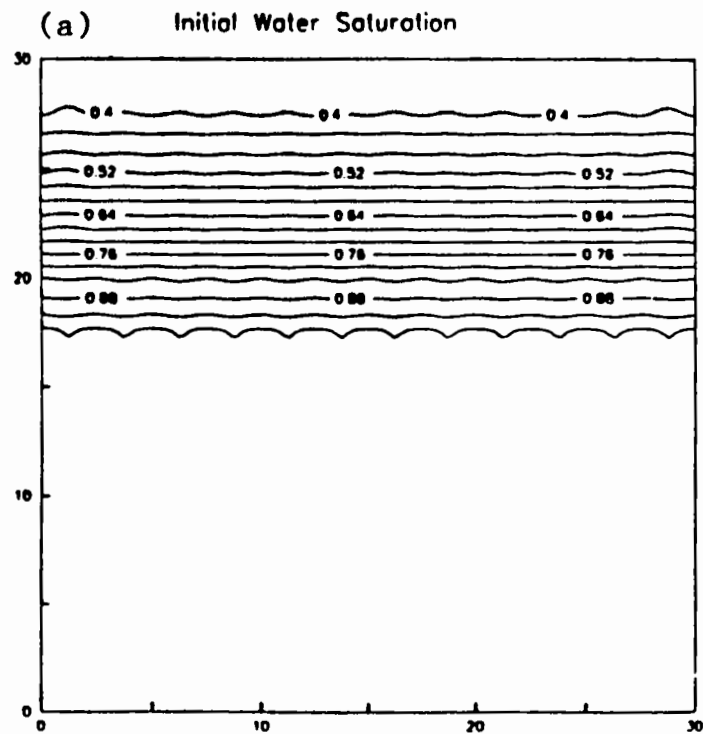
**Figure 2. Initial Water Saturation and Electrical Conductivity Distribution in 2D Sandbox From Multiphase Model Simulation**

(a) Water Saturation at t = 0.4 hr

(b) PCE Saturation After Spill, t = 0.4 hr
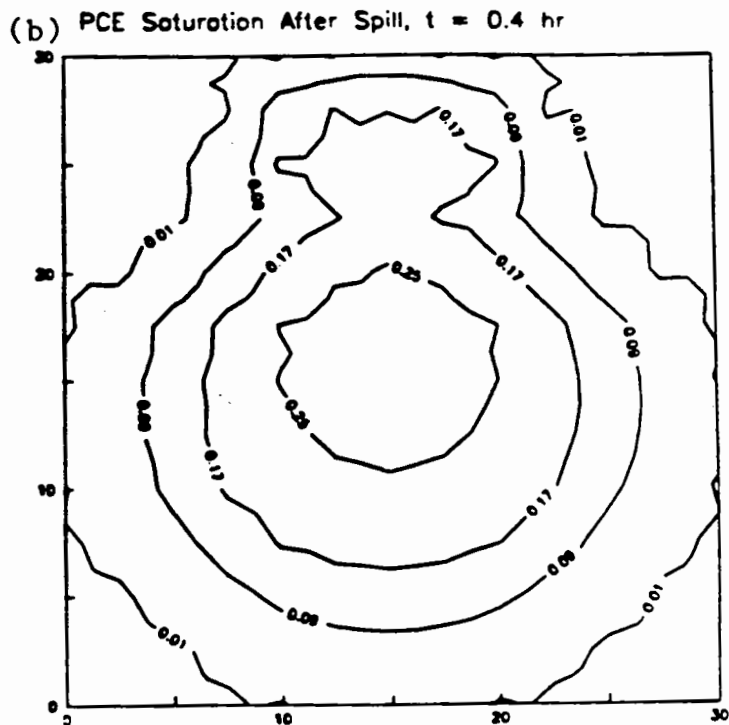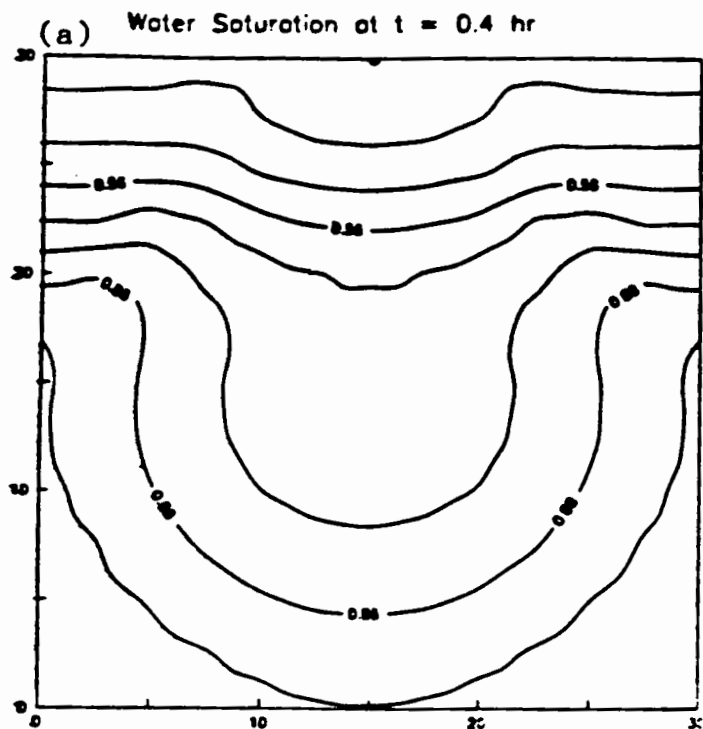
(c) Conductivity After PCE Spill (s/cm), t = 0.4 hr
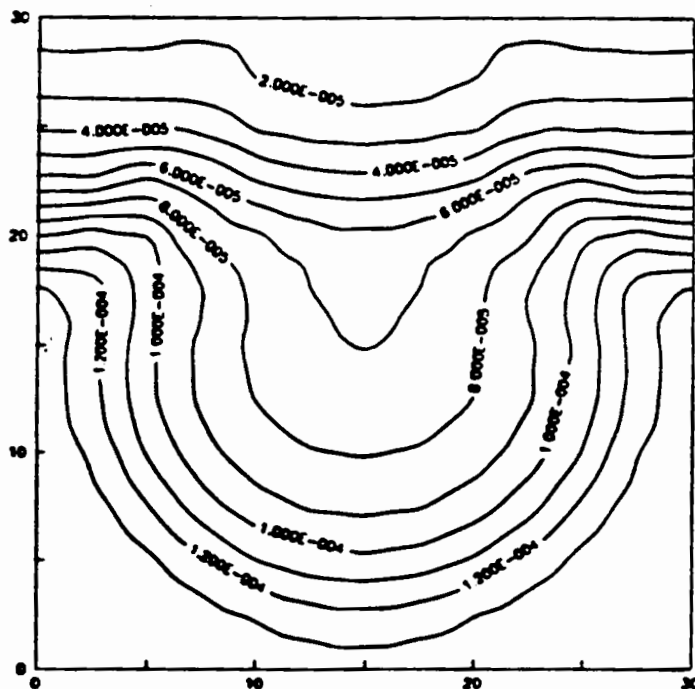
Figure 3. (a) Water Saturation, (b) PCE Saturation, (c) Electrical
Conductivity Distribution at 0.4 hr After PCE Spill Started
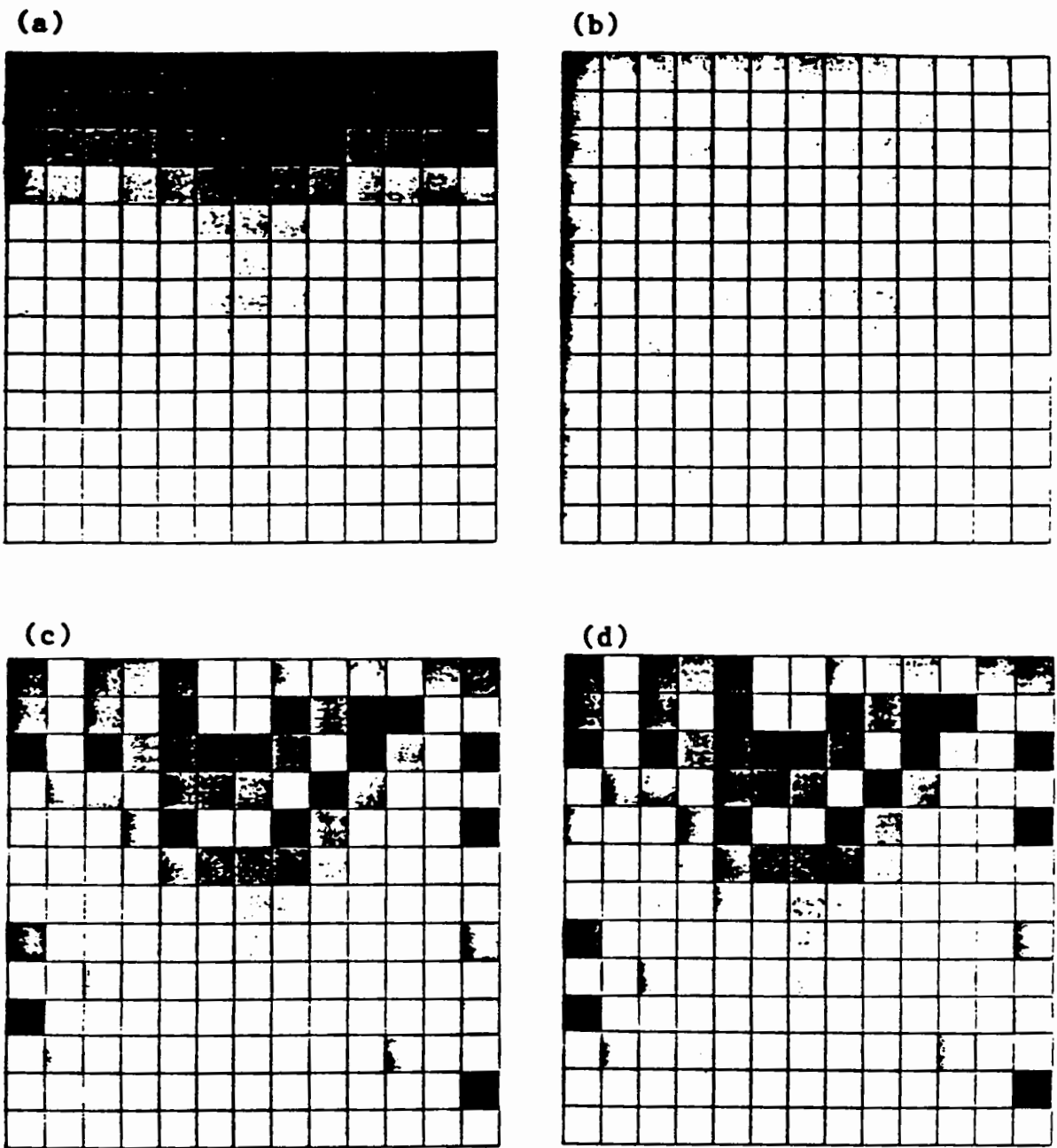
**Figure 4. Progress of EIT Inversion, (a) Original, (b) Initial Guess, (c) After 10th Iteration, (d) After 27th Iteration**
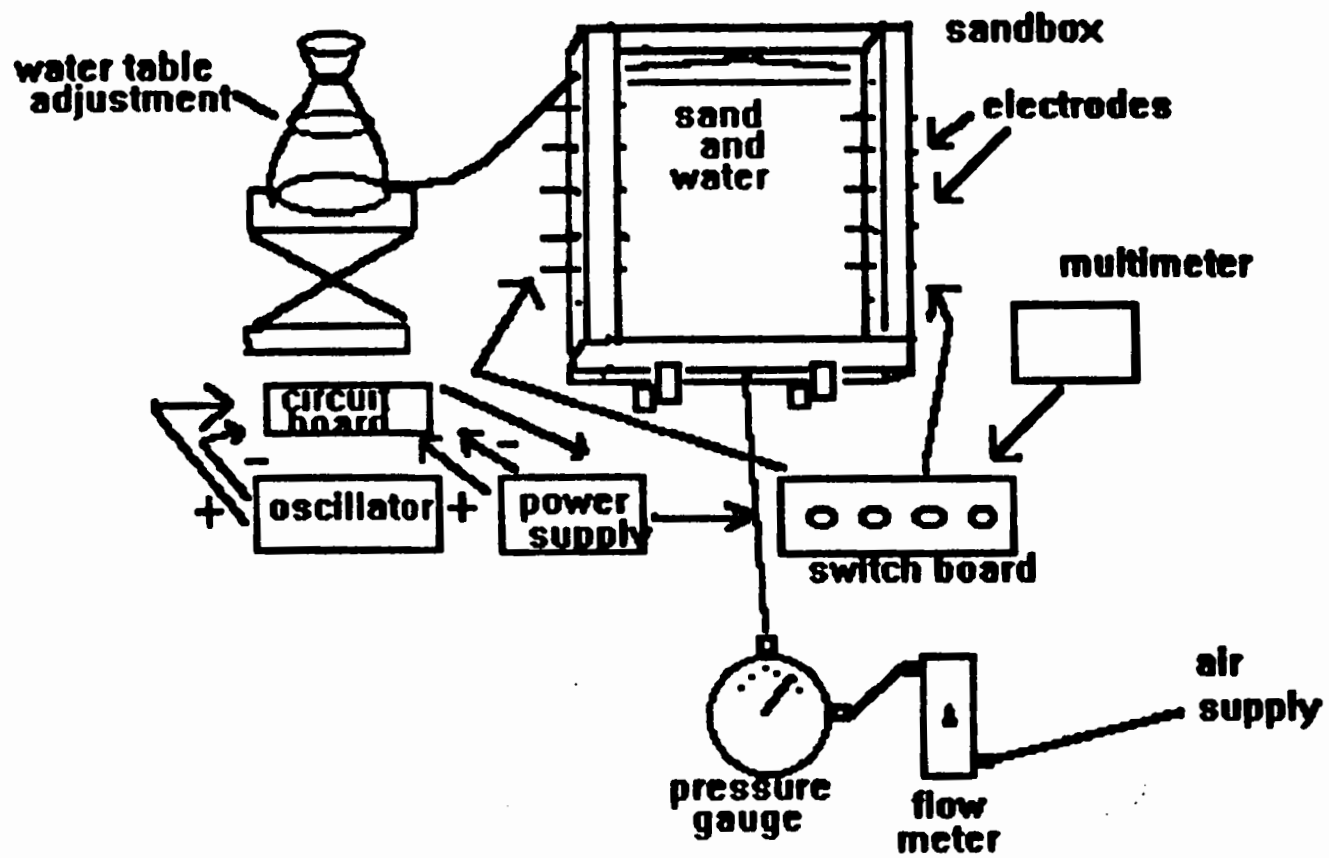
**Figure 5. Schematic Diagram of 2D Sandbox Experimental System**

‖‖‖‖‖‖‖‖‖‖‖‖‖‖‖‖‖‖‖‖
PB96-170451

# TECHNICAL REPORT DATA

| 1. REPORT NO. EPA/600/A-96/022 | 2. | 3. RECIPIENT'S ACCESSION NO. |
|---|---|---|
| 4. TITLE AND SUBTITLE<br>AIR SPARGING EXPERIMENTS ON A TWO DIMENSIONAL SAND BOX WITH DNAPLS: MULTIPHASE INVESTIGATION WITH ELECTRICAL IMPEDANCE TOMOGRAPHY | | 5. REPORT DATE |
| | | 6. PERFORMING ORGANIZATION CODE |
| 7. AUTHOR(S)<br>JONG SOO CHO | | 8. PERFORMING ORGANIZATION REPORT NO. |
| 9. PERFORMING ORGANIZATION NAME AND ADDRESS<br>USEPA<br>NATIONAL RISK MANAGEMENT RESEARCH LABORATORY<br>SUBSURFACE PROCESSES AND REMEDIATION DIVISION<br>P.O. BOX 1198<br>ADA, OK 74820 | | 10. PROGRAM ELEMENT NO. |
| | | 11. CONTRACT/GRANT NO.<br>IN-HOUSE   RSJC3 |
| 12. SPONSORING AGENCY NAME AND ADDRESS<br>USEPA<br>NATIONAL RISK MANAGEMENT RESEARCH LABORATORY<br>SUBSURFACE PROCESSES AND REMEDIATION DIVISION<br>P.O. BOX 1198<br>ADA, OK 74820 | | 13. TYPE OF REPORT AND PERIOD COVERED |
| | | 14. SPONSORING AGENCY CODE<br>EPA/600/15 |

| 15. SUPPLEMENTARY NOTES |
|---|

16. ABSTRACT

Electrical impedance tomography (EIT) applications in detection of organic chemical sources and monitoring subsurface environments during air-sparging were studied. The development of an inverse solution program and experimental tests in the laboratory were included in this study. The inverse solution model used the Newton-Raphson method with the Marquadt regularization technique. A multiphase flow and transport model was utilized to test the EIT inverse modeling. Tetrachloroethylene(PCE)infiltration was simulated with a multiphase flow model and the ability of EIT to trace the PCE distribution was tested. Computational progress of the inverse solution was presented with a graphical display of electrical conductivity distributions. The inverse program for EIT was used to obtain the electrical conductivity distribution in a 2-D sand box. The experiments included a spillage of dense non-aqueous phase liquid(DNAPL) dyed with a hydrophobic dye at the top of the sand box filled with water and air sparging from the bottom. Electrical conductivity changed in the soil as water was replaced with DNAPL or air. This made the tomographic pictures of electrical conductivity. The vapor concentration of DNAPL in the extracted air was measured with a GC to estimate the removal rate during air sparging. The tomographic images from the EIT were compared with photographic images of dyed PCE in the water filled space.

| 17. | KEY WORDS AND DOCUMENT ANALYSIS | |
|---|---|---|
| A.          DESCRIPTORS | B. IDENTIFIERS/OPEN ENDED TERMS | C. COSATI FIELD, GROUP |
| DNAPL<br>MULTIPHASE FLOW<br>AIR-SPARGING<br>EIT | | |

| 18. DISTRIBUTION STATEMENT<br><br>RELEASE TO THE PUBLIC | 19. SECURITY CLASS(THIS REPORT)<br>UNCLASSIFIED | 21. NO. OF PAGES<br>20 |
|---|---|---|
| | 20. SECURITY CLASS(THIS PAGE)<br>UNCLASSIFIED | 22. PRICE |

EPA FORM 2220-1 (REV.4-77)     PREVIOUS EDITION IS OBSOLETE